

Age-dependent changes in the gut environment restrict the invasion of the hindgut by enteric neural progenitors

Noah R. Druckenbrod^{1,2} and Miles L. Epstein^{1,*}

The enteric nervous system (ENS) develops from neural crest cells (NCCs) that enter the foregut and hindgut to become enteric neural-crest-derived cells (ENCCs). When these cells of neural crest origin fail to colonize the terminal hindgut, this aganglionic region becomes non-functional and results in a condition in humans known as Hirschsprung's disease (HSCR). One of the genes associated with HSCR is endothelin receptor type B (*Ednrb*). To study the development of colonic aganglionosis we have utilized a novel knockout mouse (*Ednrb^{flex3/flex3}*), in which the expression of a null *Ednrb* allele and YFP is confined to NCCs. We have identified two primary cellular defects related to defective EDNRB signaling. First, ENCC advance in *Ednrb^{flex3/flex3}* embryos is delayed shortly after NCCs enter the gut. Apart from this early delay, *Ednrb^{flex3/flex3}* ENCCs advance normally until reaching the proximal colon. Second, as *Ednrb^{flex3/flex3}* ENCCs reach the colon at E14.5, they display migratory defects, including altered trajectories and reduced speed, that are not dependent on proliferation or differentiation. We constructed grafts to test the ability of donor ENCCs to invade a recipient piece of aganglionic colon. Our results indicate that the age of the recipient, and not the age or genotype of donor ENCCs, determines whether the colon is invaded. We identify changes in laminin expression that are associated with the failure of ENCCs to invade recipient tissue. Together, our data suggest that a defect in pre-enteric *Ednrb^{flex3/flex3}* NCCs results in delayed colonic arrival, which, due to environment changes in the colon, is sufficient to cause aganglionosis.

KEY WORDS: Hirschsprung's disease, Endothelin receptor B, Multicellular invasion, Neural crest cells, Time-lapse microscopy, Tissue graft, Cre-lox, Colon, Mouse

INTRODUCTION

The enteric nervous system (ENS) is formed primarily from neural crest cells (NCCs) from the post-otic hindbrain (vagal NCCs) and by a smaller contribution from the sacral neural tube (sacral NCCs) (Burns et al., 2000). Vagal NCCs migrate to the anterior portion of the fetal gut and enter the pharynx to become enteric neural crest-derived cells (ENCCs). ENCCs subsequently advance caudally as multicellular strands along the entire length of the developing gut. The resulting network of ganglia controls motor activity, secretory functions and microcirculation, and regulates immune and inflammatory responses in the gastrointestinal tract. When the ENS is absent from a gut region, the gut loses motor coordination and undergoes sustained contraction. The absence of such ganglia from the human distal colon is a diagnostic feature of Hirschsprung's disease (HSCR). Cases of HSCR are most frequently associated with mutations affecting RET or endothelin receptor type B (EDNRB) signaling (McCallion and Chakravarti, 2001), but HSCR is also associated with mutations in a number of other genes (McCallion et al., 2003; Gershon and Ratcliffe, 2004; Anderson et al., 2006; Heanue and Pachnis, 2007).

HSCR results from the failed advance of ENCCs through the hindgut, but the cellular and molecular defects resulting in colonic aganglionosis are not clear. Normal ENS development initially proceeds with the production of a sufficient pool of neural crest progenitor cells capable of advancing into the foregut. Aganglionosis results when an inadequate number of pre-enteric NCCs are generated either experimentally by neural tube ablation and/or grafting (Yntema

and Hammond, 1954; Peters van der Sanden et al., 1993; Barlow et al., 2008) or genetically by mutation (Kapur et al., 1996; Maka et al., 2005; Stanchina et al., 2006). Once in the gut, aganglionosis can also result from ENCC defects in proliferation (Sidebotham et al., 2002; Young et al., 2005; Landman et al., 2007; Simpson et al., 2007) and/or differentiation (Young et al., 2004; Anderson et al., 2006). Defects in ENCC migration can also cause aganglionosis (Breau et al., 2006). The migratory properties of ENCCs in situ has been studied by tracking ENCCs in fetal mouse gut (Young et al., 2004; Druckenbrod and Epstein, 2005) or individually labeled ENCCs in chick gut (Druckenbrod and Epstein, 2007). However, it has been difficult to determine the intrinsic migratory capability of individual ENCCs independent of the influence of proliferation and differentiation, or the local gut microenvironment through which they advance.

Much of our information on HSCR comes from studies of animal models. There are multiple mouse genes, which, when mutated, result in aganglionosis restricted to the colon (Lane, 1966; Webster, 1973; Baynash et al., 1994; Herbarth et al., 1998; Hosoda et al., 1994; Yanagisawa et al., 1998; de Graaff et al., 2001; Breau et al., 2006). Two mouse models that have been used extensively and closely resemble the human phenotype are piebald-lethal mice that lack *Ednrb* expression (*Ednrb^{sl/sl}*) and lethal-spotted mice that lack *Edn3* expression (*Edn3^{ls/ls}*) (Hosoda et al., 1994; Baynash et al., 1994; Garipey et al., 1998). Studies have found associated defects in *Edn3^{ls/ls}* ENCCs, including decreased proliferation, increased differentiation and reduced expression of the neural crest stem cell marker SOX10 (Barlow et al., 2003; Bondurand et al., 2006). Other studies have found changes in the gut environment associated with aganglionosis. In *Edn3^{ls/ls}* mice, increased laminin is found in aganglionic colons, a result suggesting that laminin reduces the number of ENCCs available for colonization by increasing ENCC differentiation (Jacobs-Cohen et al., 1987; Wu et al., 1999). Despite these studies, the cellular defects responsible for the failure of ENCC advance into the hindgut remain unknown.

¹Department of Anatomy and Neuroscience Training Program, University of Wisconsin School of Medicine and Public Health, Madison, WI 53705, USA.

²Department of Neurology, Harvard Medical School, Boston, MA 02115, USA.

*Author for correspondence (mepstein@wisc.edu)

To date, the properties and migratory behavior of ENCCs along the colon during the last stages of colonization have not been directly examined in HSCR animal models. In order to further our understanding of failed ENCC advance in the hindgut, we studied ENS development in mice with an NCC-specific deletion of *Ednrb* (*flex3* allele). Control heterozygous mice (*Ednrb^{flex3/+}*) are viable and phenotypically indistinguishable from wild-type pups or fetuses (Druckebrodt et al., 2008). However, mutant homozygous pups (*Ednrb^{flex3/flex3}*) show the characteristic aganglionic colon of HSCR and die within 5 weeks from megacolon. We utilized NCC-specific expression of YFP to isolate and visualize the in situ properties of mutant ENCCs in gut fated to become aganglionic (Danielian et al., 1997; Srinivas et al., 2001; Druckebrodt and Epstein, 2005). We investigated ENCC proliferation, differentiation and migration in *Ednrb^{flex3/+}* and *Ednrb^{flex3/flex3}* fetuses, referred to as control and mutant, respectively, throughout the remainder of the text. Our data indicate that mutant ENCCs are delayed in their advance along the gut by almost 24 hours relative to wild-type or control preparations. Apart from this delay, mutant ENCCs migrate at similar individual speeds to their control counterparts until they reach the proximal colon at E14.5, when they begin to display defective migratory behavior that is independent of cell proliferation or differentiation. We constructed tissue grafts to determine whether the defect was located in the ENCCs or the aganglionic colon. Our results suggest that a time-dependent change in the mutant hindgut environment restricts ENCC migration and that this delayed ENCC advance is sufficient to result in colonic aganglionosis in mutant gut.

MATERIALS AND METHODS

Animals

The following transgenic and recombinant mice were bred on a C57BL/6 background: *Tg^{Wnt1-Cre}* (Danielian et al., 1997), *Rosa26^{YFPStop}* (Srinivas et al., 2001) and *Ednrb^{flex3}* (Druckebrodt et al., 2008). Mice with the genotype *Tg^{Wnt1-Cre/+}Ednrb^{flex3/+}* were bred with mice containing *Rosa26^{YFPStop}Ednrb^{flex3/flex3}* alleles to generate fetuses and animals with YFP-positive NCCs lacking EDNRB. Mice and fetuses were genotyped by PCR as described previously (Druckebrodt and Epstein, 2005; Druckebrodt et al., 2008). Timed mating was carried out; pregnant mice were killed by cervical dislocation after treatment with isoflurane and the day of the vaginal plug was considered as embryonic day (E) 0.5. The University of Wisconsin Animal Care Committee approved these procedures.

Organ culture

The gastrointestinal tracts from YFP-positive fetuses were placed in culture media [DMEM/F12 (Cellgro), heat-inactivated 10% FBS (Gibco), 2 mM L-glutamine (HyClone), 50 mM D-glucose, 30 mM NaHCO₃, 50 U penicillin, 50 µg streptomycin; pH 7.4] and incubated in 5% CO₂ at 37°C. The EDNRB antagonist BQ-788 (American Peptide) was constituted in DMSO and used at 5–10 µM. Time-lapse imaging was done as described previously (Druckebrodt and Epstein, 2005).

Tissue grafts

Culture dishes were filled with 2% agarose prepared by diluting melted 4% agarose in water with an equal volume of culture media, and were equilibrated in media for 12 hours at 37°C. Media was removed and a small

piece of black Millipore paper was placed on the gel. Previously identified donor and recipient colon were cut with a tungsten needle, and the cut ends were quickly placed in apposition on top of the filter paper in their correct rostral-caudal orientation. Donor segments were cut near the wavefront. After 1–2 hours of incubation at 37°C, media was added to the dishes. The next day, steel pins were used to secure the distal ends of the grafted segments. After 6 days, cultures were fixed and immunostained for YFP. The lengths of each continuous YFP strand extending from the graft site were measured and averaged. To measure the area of grafted cells (Fig. 3B) and the percentage of Hu-positive cells (Fig. 5), equal thresholds were set for the YFP signal and were used to produce a binary mask for quantification.

Cell and image analysis

Cell speeds were the average distance each single ENCC (isolated or at the front of a strand) moved over 7- to 14-minute intervals for 2–14 hours. On average, each age/genotype pair contained 35 tracks and 1253 data points. Directionality is the length of a line between the start and end of each track divided by the actual length of the track based on the 7- to 14-minute positional plots, whereby 1 represents a straight-line path. Directionalities were averaged for each condition. Wavefront advance is the change in position of the most caudal ENCC strand before and after 12 hours of incubation at 37°C in 5% CO₂. Images were processed and analyzed with Metamorph (Molecular Devices), ImageJ (NIH), SigmaPlot (Systat Software) and Excel (Microsoft). Adobe Photoshop was used to create montages, and to add color and symbols.

Immunohistochemistry

Whole-mount tissue was fixed in 4% paraformaldehyde for 1–2 hours, treated with 1% Triton X-100, washed and incubated overnight with primary, and then secondary, antibodies. For sections, tissue was equilibrated in OCT Compound, frozen on dry ice and sectioned at 20 µm on a cryostat. Immunostained tissues were imaged with a Bio-Rad MRC 1024 confocal microscope. Primary and secondary antibodies are listed in Table 1.

Semi-quantitative RT-PCR

Total RNA from purified ENCCs was isolated using RNeasy Protect Mini Kit (Qiagen). RNA (100 ng) was primed with *Ednrb*-specific primers: forward, 5'-ACCGTGGTTTAAACGCCATAG-3'; reverse, 5'-CAGCTC-TCTCGGAGGCATAC-3' (Integrated DNA), and transcribed with SuperScript II Reverse Transcriptase (Invitrogen). The same primers were used for end-point PCR, using a cDNA template and transcribed by Taq polymerase (New England Biolabs), and products were run on a 15% acrylamide gel stained with ethidium bromide.

Cell sorting

Gastrointestinal tracts were removed from YFP-positive E14.5 animals and identified as *Ednrb^{flex3/+}* or *Ednrb^{flex3/flex3}* by the location of the ENCC wavefront. Tissues were dissociated in a mixture of 5 mg/ml collagenase type III (Worthington Biochemicals) and 2 mg/ml DNase type I (Sigma) for 10–20 minutes at 37°C, centrifuged at 100 g, washed in PBS and triturated with fire-polished siliconized glass pipettes of decreasing diameter. Dissociates were centrifuged at 100 g, resuspended in DMEM/F12 buffered with HEPES, filtered through 20 µm Nitex and sorted into YFP-positive and -negative pools with a Becton Dickinson Vantage SE fluorescence activated cell sorter. The sorted cells were collected at 4°C in siliconized tubes and were then prepared for isolation of RNA or immunostaining.

Table 1. Antibodies used in this study

Primary antibody	Manufacturer	Dilution	Secondary antibody*
Chicken anti-GFP	Aves Labs (San Francisco, CA, USA)	1:1000	Donkey anti-chick Cy2
Human anti-Hu	Epstein lab (Madison, WI, USA)	1:1000	Goat anti-human Cy3
Rabbit anti-EDNRB	Santa Cruz Biotechnology (Santa Cruz, CA, USA)	1:200	Goat anti-rabbit Cy3, HRP
Rat anti-BrdU	Abcam (Cambridge, MA, USA)	1:50	Donkey anti-rat Cy5
Rabbit anti-laminin	Sigma (St Louis, MO, USA)	1:500	Goat anti-rabbit Cy3

*All secondary antibodies are from Jackson ImmunoResearch (West Grove, PA, USA).

BrdU incorporation

To study the proliferation of ENCCs, BrdU (10 mg/ml) was injected intraperitoneally into pregnant mice at a dose of 50 μ g/g of body weight. E14.5 fetuses were harvested 2-3 hours after injection and YFP-positive guts were dissociated as described above. The dissociated cells were fixed and then immunostained for YFP and BrdU. Cells were sorted and counted using an LSRII Becton Dickinson benchtop analyzer.

RESULTS

We developed a novel knockout mouse in which the expression of a null *Ednrb* allele and yellow fluorescent protein (YFP) is confined to NCCs. To make the null allele (*flex3*), exon 3 of *Ednrb* was flanked by loxP sequences and was selectively excised by Cre recombinase (Druckenbrod et al., 2008). In order to excise *Ednrb* specifically in ENCCs, Cre recombinase expression was regulated by the *Wnt1* promoter (*Tg^{Wnt1-Cre}*), which is activated specifically in NCCs prior to their emigration from the neural tube (Danielian et al., 1997; Jiang et al., 2000). In addition, we bred *Ednrb^{flex3}* mice with transgenic mice that constitutively express YFP (*Rosa26^{YFPStop}*) in the presence of Cre recombinase (Srinivas et al., 2001). Mating these lines of mice enabled us to obtain animals with the *Ednrb* mutation confined to NCCs, which in turn are all fluorescent.

To confirm *Ednrb* disruption in ENCCs, YFP-positive (i.e. ENCCs) and YFP-negative (i.e. smooth muscle precursors and enterocytes) cells were isolated by FACS from *Ednrb^{flex3/+}* and *Ednrb^{flex3/flex3}* tissue for RT-PCR. RT-PCR of a sequence within *Ednrb* exon 7 produced a product using template cDNA derived from *Ednrb^{flex3/+}*, but not *Ednrb^{flex3/flex3}*, ENCCs (Fig. 1). Immunostained E15.5 gut cross-sections showed that YFP-negative smooth muscle progenitors in *Ednrb^{flex3/+}* and *Ednrb^{flex3/flex3}* gut both contain EDNRB, and that only *Ednrb^{flex3/+}* ENCCs colocalize with EDNRB (Fig. 2). Together, these data and previous findings (Druckenbrod et al., 2008) indicate that EDNRB is deleted specifically in *Ednrb^{flex3/flex3}* ENCCs.

Ednrb^{flex3/flex3} ENCC migration is delayed early in development

To characterize the development of the aganglionosis, we measured ENCC advance through control *Ednrb^{flex3/+}* and mutant *Ednrb^{flex3/flex3}* gut from E10.5 to E14.5 (Fig. 3). At E10.5, mutant ENCCs were reduced in number, were not as caudally advanced and were less dense compared with the corresponding regions of control gut. Occasionally there were no ENCCs in E10.5 mutant gut (data not shown). Between E10.5 and E11.5, mutant ENCCs increased in number and in their advance, but remained ~24 hours behind those in identically aged control gut. In contrast to controls, mutant ENCCs did not invade the cecal body in their initial advance but did so later in development (Fig. 3D; see Movies 1 and 2 in the supplementary material). By E14.5, the control ENCC wavefront had reached the terminal hindgut, whereas the mutant wavefront had reached only the proximal colon. The absence of ENCCs in the mutant hindgut allowed us to identify sacral neural crest cells and extrinsic nerve fibers, which are normally obscured and indistinguishable from vagal neural crest from E14.5 onwards (Fig. 3D, inset). Although the number of sacral-derived crest cells was small, at E14.5 they extended rostrally in the mutant hindgut. In the fetal gut, sacral crest cells are made up of long, thin strands that project rostrally and contain fewer, more widely spaced cell bodies than do strands from the vagal crest. It is not clear what properties result in their advance or failed expansion, but recent studies suggest a difference in RET expression between vagal- and sacral-derived neural crest may be crucial (Delalande et al., 2008).

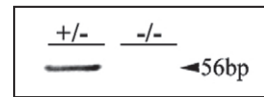


Fig. 1. *Ednrb* mRNA expression in control and mutant gut. RT-PCR of mRNA isolated from FACS-purified YFP-positive ENCCs from control (*Ednrb^{+/+}*) and mutant (*Ednrb^{-/-}*) mice. Only control ENCCs contain RNA recognized by *Ednrb* primers (giving a 56 bp product).

Time-lapse recordings of control and mutant ENCCs were made to determine whether differences existed in their speed or directionality through similar gut regions, and separate experiments were performed to measure the change in wavefront position after 24 hours in culture (see Fig. S1A-C in the supplementary material). The only significant difference found between E10.5 and E14.5 was the reduced speed of mutant ENCCs near the cecal base. This difference could relate to the lack of EDNRB, or to the fact that mutant ENCCs do not directly invade the cecum. The overall absence of differences in speed and directionality seems surprising but is consistent with previous findings that indicate wavefront advance occurs at a relatively constant rate once a critical number of ENCCs is reached (Young et al., 2004; Druckenbrod and Epstein, 2005).

Mutant ENCCs migrate aberrantly in post-E14.5 colon

At E14.5, an age when both wild-type and *Ednrb^{flex3/+}* guts are fully occupied by ENCCs, we find that mutant ENCCs begin to display behaviors that indicate a defective advance. As E14.5 mutant ENCCs advanced through the proximal colon, their network became denser but had more narrow strands compared with those in control gut (Fig. 4). Instead of following the general rostral-caudal trajectory found in wild-type and *Ednrb^{flex3/+}* colon (Fig. 4A,C; see Movie 3 in the supplementary material), most mutant ENCCs migrated along paths perpendicular to the rostral-caudal axis of the gut (Fig. 4B,D; see Movies 4 and 5 in the supplementary material). A few strands advanced caudally, but these also displayed reduced speed and had

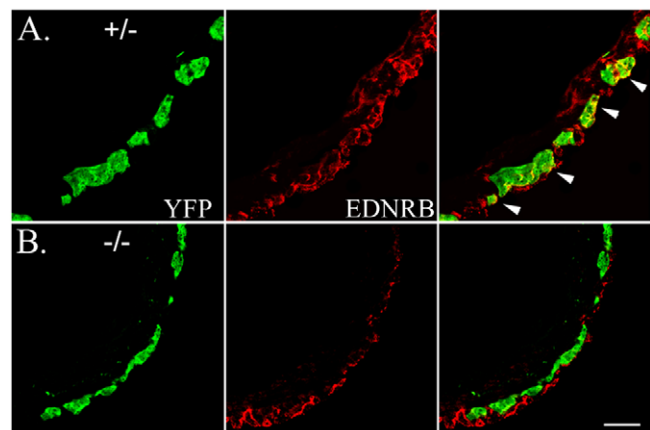


Fig. 2. EDNRB and YFP immunostaining of cross-sections from E15.5 control and mutant proximal colon. (A) EDNRB (red) in control tissue colocalizes with YFP-positive ENCCs (green; colocalization in overlay is yellow). A few prominent regions of colocalization are indicated by arrowheads. (B) EDNRB staining in mutant tissue is seen in smooth muscle but EDNRB does not colocalize with YFP-positive ENCCs. Scale bar: 50 μ m.

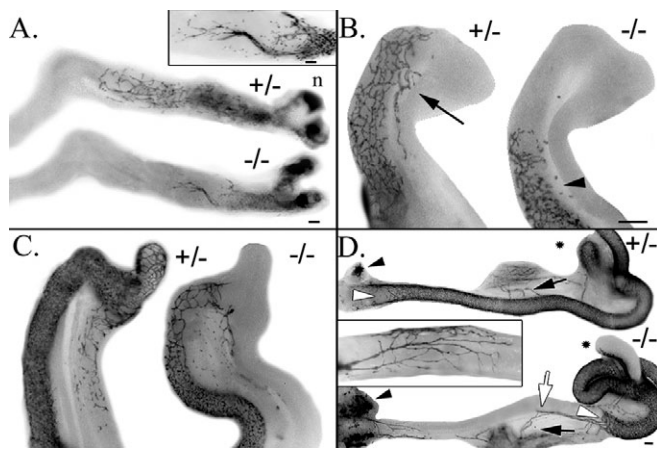


Fig. 3. Position of YFP-positive ENCCs in control and mutant gut from E10.5-E14.5. YFP-positive ENCCs are visible as dark puncta and strands. **(A)** The wavefront in E10.5 control gut (top) extends to the mid-ileum, whereas the wavefront in the mutant (bottom) contains fewer ENCCs and just extends to the proximal small intestine. The two anterior dark ovals (indicated by 'n') are the nodose ganglia. Inset: high magnification of mutant foregut shows that many of the delayed ENCCs have not yet formed strands. **(B)** The wavefront in E11.5 controls (left) extends to the cecum and proximal colon, whereas in the mutant (right), the wavefront remains in the ileum. Note the ENCCs that traverse the mesentery between the ileum and colon (arrow and arrowhead in control and mutant, respectively). **(C)** At E12.5, ENCCs in control gut (left) advance through the proximal colon or remain in the distal colon as isolated clusters. The ENCC wavefront in the mutant gut (right) is only at the proximal cecum but ENCCs form a strand into the proximal colon and are absent from the cecal body. **(D)** At E14.5, the wavefront in control gut (top) has reached the terminal portion of the colon (white arrowhead), whereas mutant ENCCs remain in the proximal colon (white arrowhead and arrow, bottom) and begin to display defective migration. Asterisk highlights the hypoganglionic mutant cecum. Black arrowheads and arrows show pelvic plexus and fibers, respectively, passing from the mesentery. Inset: high magnification of sacral-derived neural crest cells and fibers within an otherwise aganglionic mutant hindgut. Scale bars: 100 μ m.

erratic trajectories (compare Fig. 4Aa with 4Bc). Quantification of these behaviors showed that mutant ENCC speed, directionality and overall wavefront advance dropped sharply at E14.5 (see Fig. S1A-C in the supplementary material). Between E15.5 and E16.5, very few ENCC strands showed detectable migration, but a few ENCCs separated from their strands and migrated erratically through the growing gut (see Fig. S2 and Movie 6 in the supplementary material).

Because the advance of the wavefront depends on maintaining the ENCC number above a certain threshold, the inability of mutant ENCCs to advance through E14.5 gut could result from impaired proliferation, premature differentiation or defective migration. To investigate whether there is a proliferative defect, we used FACS cytometry on E14.5 gut taken from BrdU-injected mothers (see Fig. S3 in the supplementary material). Although the average number of ENCCs in the E14.5 mutant was 43% ($\pm 2.5\%$) of those counted in control small and large intestine, BrdU experiments revealed no significant differences between control and mutant ENCC proliferation at E14.5, the stage at which mutant ENCC advance becomes defective. To investigate whether mutant ENCCs were prematurely differentiating, we compared the organization and percentage of ENCCs expressing the pan-

neuronal marker Hu at the wavefront of control and mutant gut (Fig. 5). The exclusive expression of neuronal Hu proteins in the cell body makes this marker useful for the enumeration of neurons. The control nascent ganglia were generally larger, and more rounded and spaced, with some regularity along strands (Fig. 5A). By contrast, mutant ganglia were smaller, poorly formed and oriented perpendicularly to the rostral-caudal axis along disconnected strands (Fig. 5B). However, no significant difference in the percentage of Hu-positive ENCCs was found between these preparations or those at earlier ages (Fig. 5C). Together, these data do not implicate altered proliferation or differentiation in the defective advance of ENCCs, which leads to aganglionosis.

EDNRB antagonist disrupts ENCC migration

Application of the EDNRB-specific antagonist BQ-788 leads to colonic aganglionosis in fetal organ cultures (Sidebotham et al., 2002; Nagy and Goldstein, 2006). Why do otherwise normally advancing ENCCs, once in the presence of BQ-788, fail to reach the terminal colon? We wanted to know if the defective advance produced by acute EDNRB inhibition occurred on the timescale of proliferation/differentiation, or whether it was associated with more rapid changes in cell behavior. Application of 5 μ M BQ-788 to E11.5-E12.5 mutant preparations did not elicit a response (data not shown). However, BQ-788 produced a pronounced dose-dependent response in wild-type ENCC morphology and migration. Upon application of 5 μ M BQ-788, wild-type ENCC strands and processes retracted, resulting in reduced motility (see Movie 7 in the supplementary material). After application of 10 μ M BQ-788, ENCCs rapidly rounded up and strands dissociated within 2 hours (Fig. 6A). After 6-12 hours, ENCCs reassociated and resumed their advance. This temporary dissociation of ENCC strands effectively delayed the wavefront and the distance it advanced over 12 hours (Fig. 6B). Therefore, application of BQ-788 results in the wavefront reaching the hindgut later than it normally would, preventing the colonization of the otherwise normal hindgut. In addition, application of BQ-788 to E10.5-E11.5 mutant preparations had no observable effect on ENCC morphology or advance, suggesting that the expression of EDNRB in ENCCs is necessary for a response to BQ-788.

Post-E14.5 colonic environment is less permissive to ENCC invasion

To determine whether the migratory defect in E14.5 mutant gut is ENCC-autonomous or mediated by the environment, we constructed grafts to compare the abilities of control and mutant ENCCs to invade aganglionic gut of different ages and genotype (Fig. 7; see Figs S4 and S5 in the supplementary material). Control donor ENCCs invaded E13.5 mutant colon extensively (Fig. 7A), and E14.5 mutant donor ENCCs showed a similar capacity for invasion when grafted to E13.5 control recipient colon (Fig. 7C). Donor ENCCs of either genotype made little or no invasion of E14.5 *Ednrb*^{flex3/flex3} colon (Fig. 7B) or older (our unpublished results). Donor ENCCs never invaded recipient gut already occupied by ENCCs, so experiments using E14.5 *Ednrb*^{flex3/+} recipient gut were uninformative (our unpublished results). These results suggest that it is the age of the recipient tissue, not the genotype, that restricts the invasion of donor ENCCs.

The nonpermissive environment is associated with changes in laminin

We propose that, after E14.5, a time-dependent change in *Ednrb*^{flex3/flex3} colon restricts invasion by ENCCs from either genotype. What accounts for the failure of ENCCs to invade post-

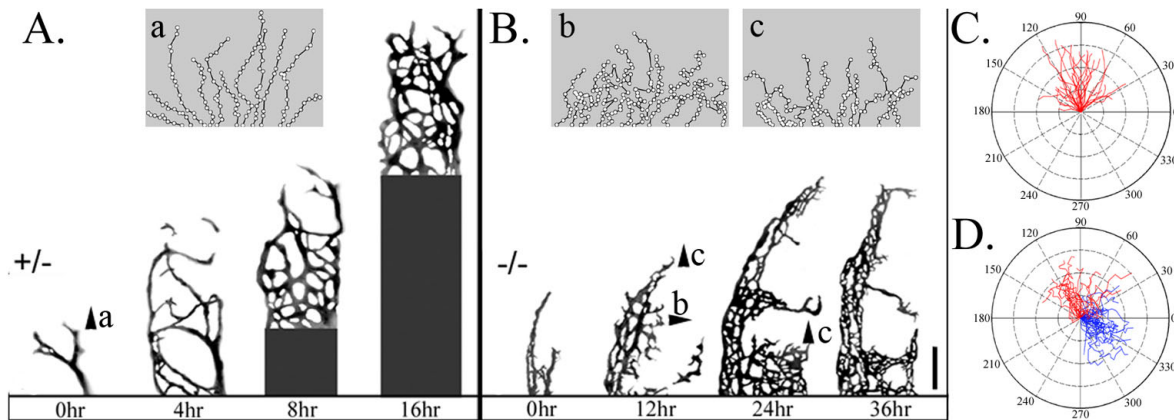


Fig. 4. Montage comparing the in situ advance of control and mutant ENCCs. (A) Typical control ENCC advance through E13.5 colon. (B) Typical mutant ENCC advance through E14.5 colon. Time (hours) is indicated. (a-c) Migratory paths of individual ENCCs marked every 7 minutes (white circles), tracked from regions corresponding to numbered arrowheads in A and B. Tracks were taken from multiple preparations and the origin of each track was placed along a line for clarity. (A) The control wavefront is made up of thick, smooth strands, with relatively large spacing between them. Here the wavefront advances at $\sim 46 \mu\text{m/hr}$ ($750 \mu\text{m}$ in 16 hours). Black rectangles cover the area that fell out of view while filming the wavefront advance. (a) The rostral-caudal migratory paths of individual ENCCs show persistent caudal paths. (B) The mutant wavefront advances at $\sim 11 \mu\text{m/hr}$ ($400 \mu\text{m}$ in 35 hours) and is made up of a denser network of narrow strands with a 'jagged' outline. The mutant wavefront is divided into 'primary' ENCCs that advance perpendicular to the rostral-caudal axis (b) and 'secondary' ENCCs that advance along the rostral-caudal pathway (c). Most of the migratory ENCCs are primary. The mutant ENCCs that do follow a rostral-caudal trajectory have a reduced speed and show a greater variability of direction (compare a and c). (C,D) The angular trajectories of individual ENCCs taken from multiple experiments in E13.5 control (C) and E14.5 mutant (D) colon. The caudal direction corresponds to 90° . The blue and red tracks correspond to 'primary' and 'secondary' mutant ENCCs, respectively. Scale bar: $100 \mu\text{m}$.

E14.5 *Ednrb*^{flex3/flex3} colon? Laminin is a candidate molecule suspected to play a role in aganglionosis (Jacobs-Cohen et al., 1987; Wu et al., 1999). To investigate the pattern and development of laminin expression in the colon, we imaged the wavefronts of control and mutant whole-mount guts from E13.5 to E14.5, the developmental window when the colon changes from a permissive to a nonpermissive environment. In E13.5 control and mutant wavefronts, laminin was sparsely distributed in punctate deposits (Fig. 8A,B). By contrast, both genotypes showed increased laminin at E14.5 (Fig. 8C,D). However, whereas the control ENCCs had reached the terminal colon, the mutant ENCCs had not. Future work will determine whether laminin has a direct role in limiting ENCC strand invasion of post-E14.5 mutant colon in situ.

DISCUSSION

Colonic aganglionosis is generally considered to be caused by defects in either NCCs or the gut microenvironment (Heanue and Pachnis, 2007; Alzahem and Cass, 2008). Our results suggest that both components underlie the disease process, with an early delay in the onset of ENCC advance and a later failure of ENCCs to invade the terminal colon. It is clear that the absence of cells within the terminal portion of the bowel can result from defects in a number of steps required for colonization of the entire gut. The process begins with the production of a sufficient pool of pre-enteric progenitor NCCs that emigrate from the neural tube to the foregut. Upon entry into the gut, the coordination of proliferation, differentiation and migration of ENCCs is required for their advance along the midgut and colon. Here we show that the *Ednrb*^{flex3/flex3} ENCC wavefront is already delayed shortly after NCCs enter the gut at E10.5, a finding suggesting that a defect limits the number of NCCs available to enter the gut. A pre-enteric NCC defect resulting in NCC apoptosis has been described for complete gut aganglionosis in SOX10-deficient

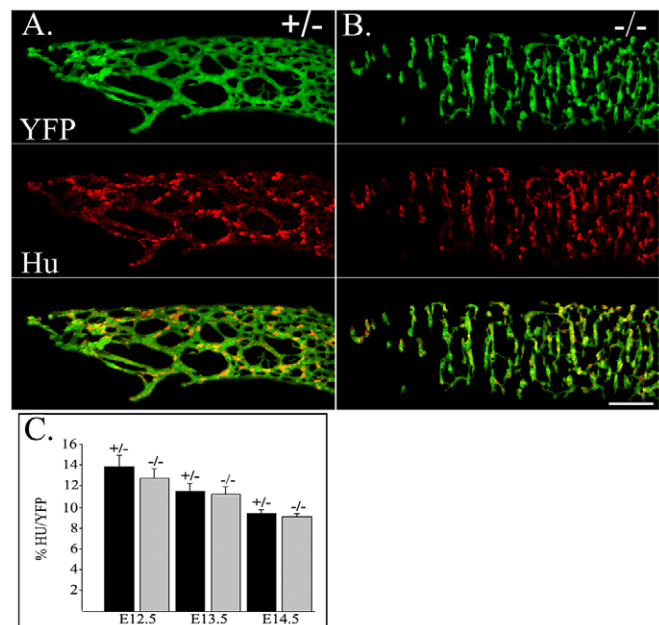


Fig. 5. Differentiation of ENCCs at the wavefront in control and mutant proximal colon. (A,B) E13.5 control (A) and E15.5 mutant (B) colon. ENCCs were immunostained for YFP (green) and Hu (red). Caudal is to the left. The mutant strands are perpendicular to the long axis of the gut and appear discontinuous, resembling the wavefront after treatment with the EDNRB antagonist. (C) To compare differentiation, the percentages of Hu- and YFP-positive ENCCs at mutant and control wavefronts from E12.5 to E14.5 were measured from multiple preparations. $n=4$ (E13.5), $n=6$ (E12.5), $n=6$ (E14.5). Error bars are s.e.m. Scale bar: $100 \mu\text{m}$.

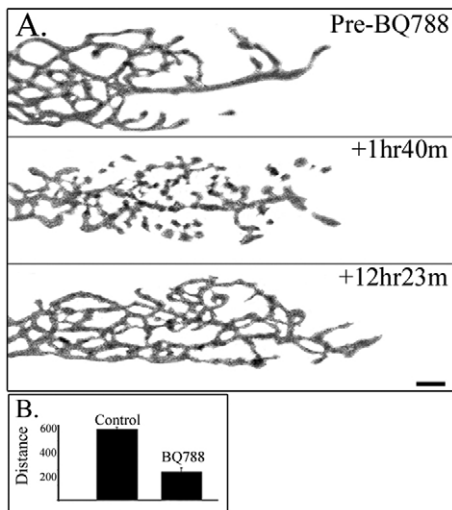


Fig. 6. The EDNRB-specific antagonist BQ-788 disrupts wild-type ENCC advance. (A) ENCCs advancing caudally (towards the right) through the E13.0 colon before and after application of $10\ \mu\text{M}$ BQ-788. Top: prior to application of the antagonist, ENCCs advance caudally and are primarily arranged as strands. Middle: ENCCs round up and largely dissociate from each other shortly after antagonist exposure. During this time, ENCCs migrate very little and do not advance caudally. Bottom: ENCCs remain dissociated for up to 12 hours but eventually reform into strands and resume caudal advance. (B) Comparison of the distance advanced by ENCCs exposed to $10\ \mu\text{M}$ BQ-788 and non-exposed controls after 12 hours. The delay produced by BQ-788 corresponds to a significantly reduced rate of advance averaged over 12 hours. $n=8$ preparations for each condition. Error bars are s.e.m. Scale bar: $100\ \mu\text{m}$.

mice (Kapur et al., 1996) and less severe colonic aganglionosis in *Sox8*, *Sox10:Edn3* and *Sox10:EdnrB* mutant mice (Maka et al., 2005; Stanchina et al., 2006). However, more subtle abnormalities in ENS development might also be associated with pre-enteric NCC defects that have not yet identified. Although delayed by ~ 24 hours, we found *EdnrB^{flex3/flex3}* mutant ENCCs still advance at equivalent speeds through the ileum and proximal colon, and it is only after they enter the proximal colon at E14.5 that migration is altered. This defective ENCC invasion is independent of their proliferation and differentiation, and is instead the result of a time-dependent change in the mutant gut microenvironment after E14.5. This change may reflect a phenomenon that occurs in the course of ENS development, so that an initial 24-hour delay in ENCC advance is sufficient to produce colonic aganglionosis.

An explanation for the failure of ENCCs to advance in the mutant colon appears to reside in the gut microenvironment, as our tissue grafting experiments revealed that both mutant and control ENCCs can invade E13.5 recipient colon of either genotype, but not E14.5 mutant recipient colon. Put simply, the age of the recipient aganglionic colon, and not the donor ENCC genotype, is crucial to ENCC invasion. This hypothesis is strengthened by our analysis that shows no change in ENCC proliferation within the intestine or differentiation at the migratory wavefront. These data differ from previous studies performed on *Edn3^{ls/ls}* mice, which also show delayed migration of ENCCs along the gut tube from E10.5 (Barlow et al., 2003). Bondurand et al. (Bondurand et al., 2006) reported regional differences in ENCC proliferation and differentiation in *Edn3^{ls/ls}*

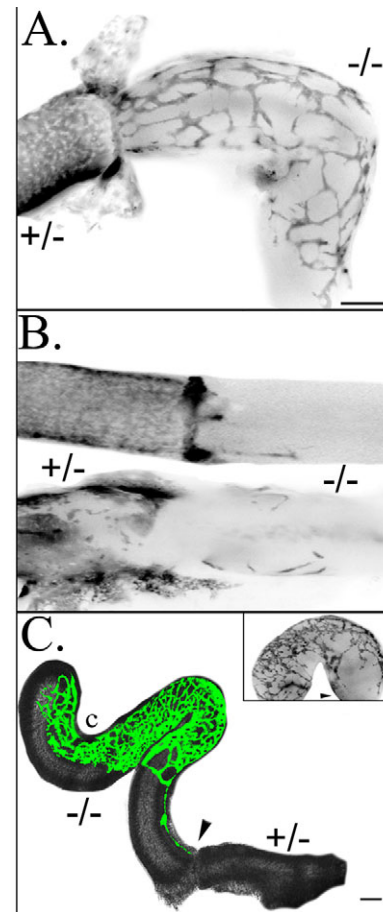


Fig. 7. Grafts showing the extent of control ENCC advance through mutant hindgut of different ages. (A) Graft between donor E13.5 control colon (left) and previously aganglionic E13.5 mutant recipient hindgut (right) after 6 days of incubation. ENCCs show extensive invasion of recipient tissue, although the most terminal portion remains uncolonized. (B) Two typical grafts between E13.5 control colon (left) and previously aganglionic E14.5 mutant recipient hindgut (right) after 6 days of incubation. ENCCs show no or very limited invasion of E14.5 hindgut. (C) ENCCs from E14.5 mutant colon invade aganglionic E13.5 control host colon. Initial positions of grafts are shown in bright-field, with mutant ENCCs superimposed in green. Arrowhead marks the junction of the two grafts and the most caudal mutant ENCC. Inset: the position of ENCCs in the host graft after 6 days of incubation reveals extensive colonization, although the terminal colon remains uncolonized (arrowhead). c, cecum. Scale bars: $180\ \mu\text{m}$.

mice. A small but significant decrease in ENCC proliferation was identified at the E11.5-E12.0 *Edn3^{ls/ls}* wavefront. Using automated cytometry, we were unable to detect any difference between mutant and control ENCCs from E14.5 dissociated gut. Small regional changes in proliferation may have gone undetected because we analyzed the BrdU-positive ENCCs as a single population. In agreement with data from Bondurand et al., we observed a reduction in ENCC number in E14.5 *EdnrB^{flex3/flex3}* gut. This reduction must be due in part to the absence of mutant ENCCs in the distal colon and cecum. However, it is also likely to reflect a decreased number of mutant NCCs entering the gut, and/or a small ongoing reduction in ENCC proliferation. With regards to neuronal differentiation, Bondurand et al. (Bondurand

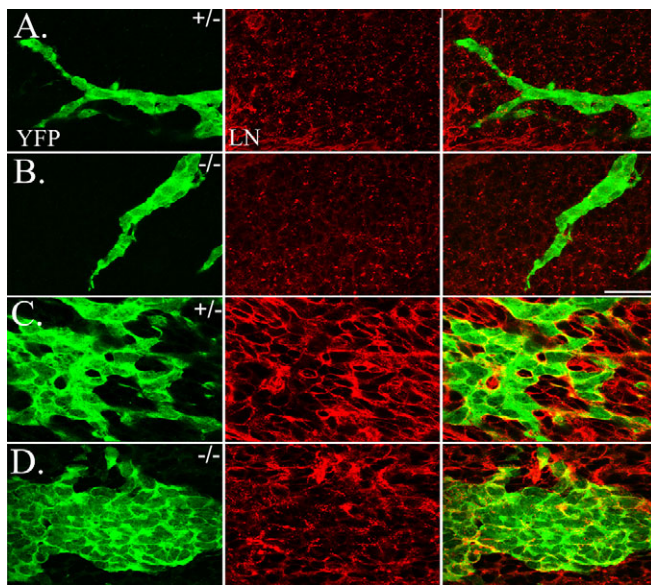


Fig. 8. Pattern of YFP and laminin expression at the E13.5 and E14.5 ENCC wavefronts of control and mutant gut whole mounts. (A,B) Laminin (LN; red) expression at E13.5 in both control (A) and mutant (B) wavefronts is sparsely distributed as punctate deposits, and little is found within advancing ENCC strands (green). (C,D) At E14.5, the density of laminin expression near the most caudal ENCCs increases in both control (C) and mutant (D) gut whole mounts. Scale bar: 50 μ m.

et al., 2006) found a 2-fold increase in the percentage of ENCCs expressing β III tubulin at the wavefront in *Edn3^{ls/ls}* compared with their wild-type counterparts, despite the fact that the neuronal differentiation within the intestines was reduced overall. By contrast, we observed no difference in the expression of the pan-neuronal marker Hu between the ENCC wavefronts of control and mutant gut. This disparity might be attributable to the properties of the two different neuronal markers used in these studies. Regardless of these changes in cell proliferation and/or differentiation, the ENCC wavefront in *Edn3^{ls/ls}* mice is still capable of advancing from E10.5 to E14.5, such that the extent of migration delay does not increase with time when compared with control guts. However, both *Edn3^{ls/ls}* and *Ednr^bflex3/flex3* hindguts fail to be colonized further by ENCCs, a result which suggests that there must be an ensuing process that prevents the wavefront from ‘catching up’ over time and invading the terminal hindgut during the remaining time in gestation (i.e. \sim 7 days in mouse and \sim 7 months in human).

Our time-lapse imaging studies provide further support for a colonic microenvironment that is nonpermissive in the E14.5 mutant. Until now, live imaging of ENCCs in intestine fated to become aganglionic had not been carried out. We found that ENCCs in E14.5 mutant colons show alterations in direction, duration and speed, and ultimately stop moving. By contrast, mutant and control ENCCs do not show any differences in these properties as they migrate in the midgut prior to E14.5. Furthermore, from E10.5 to E14.5 the difference in the position of control and mutant ENCCs remains separated by a 24-hour gap and thus does not change with developmental age. Although these data do not distinguish between a defect in the ENCCs or the gut environment, they do invite a comparison of our results with those

of Breau et al. (Breau et al., 2006). Their mice that lack β 1 integrin expression specifically in NCCs show a delay in ENCC migration that is independent of cell survival, proliferation and differentiation. This finding is instructive because they concluded that aganglionosis resulted from an ENCC defect, leading to increased aggregation and consequently a reduced ability to migrate. However, in contrast to our mutants, the difference in the position of the wavefront between the mutant and control guts does increase with fetal age, and mutant ENCCs migrate shorter distances in grafts than controls. These differences support the idea that ENCCs lacking β 1 integrin fail to invade the colon because they have reduced migratory capability, whereas ENCCs lacking EDNRB fail to colonize the *Ednr^bflex3/flex3* hindgut because of the environment.

Our experiments suggest that a change within the mutant microenvironment beyond E14.5 restricts the continued migration of ENCCs and eventually results in colonic aganglionosis. The studies of others (e.g. Wu et al., 1999) have implicated laminin as a molecule with a putative inhibitory role in the colonization of the hindgut in *Edn3^{ls/ls}* mice. We found no difference in the expression of laminin between E13.5 control and mutant colons. Rather, laminin increased between E13.5 and E14.5 in both control and mutant hindgut, a finding which suggests a role for laminin in restricting ENCC strand invasion of post-E14.5 colon. These data imply that the temporal change in permissiveness to ENCC invasion within the colonic microenvironment might not just be restricted to the mutant gut but might be a phenomenon that occurs during normal development. Further studies will need to be performed to see whether this is indeed the case, and to determine if laminin acts directly on ENCCs to alter their invasion of the gut wall.

A link between the delay in ENCC migration and aganglionosis comes from experiments combining in situ time-lapse analysis with the EDNRB-specific antagonist BQ-788. Application of BQ-788 to cultured mouse and chick preparations results in aganglionic colon. We found that the antagonist elicited a pronounced migratory and morphological response from wild-type, but not mutant, ENCCs. These responses ultimately caused a temporary cessation of ENCC advance. The rapidity of the response argues for an effect on migration rather than proliferation or differentiation. In addition, the resulting aganglionosis following BQ-788 treatment of wild-type gut suggests that the same time-dependent changes restricting ENCC entry in mutants are likely to occur in control colon. The molecular role of EDNRB signaling in ENCC strand invasion and its failure in the mutant are unknown. However, studies in cancer cells may prove to be informative. For example, interaction and communication between advancing melanoma cells is disrupted by an EDNRB-specific antagonist (Bagnato et al., 2004; Lahav, 2005), whereas EDNRB signaling counteracts cell dissociation in vitro by regulating focal adhesion and cytoskeletal molecules (Lange et al., 2007). Therefore, changes in ENCC morphology and migration following BQ-788 application to wild-type colon might result from alterations in the ability of ENCCs to associate with one another. It is unknown how the effect produced by acute pharmacological inhibition of EDNRB signaling relates to the absence of EDNRB seen in transgenic mice. Future experiments will be necessary to clarify the mechanism behind the effect of BQ-788 on ENCC behavior.

Although the mutant vagal ENCCs fail to reach the terminal hindgut, the mutant sacral-derived neural crest cells are present at E14.0 (Fig. 3). Their number is initially small and does not appear to increase substantially. The fate of these sacral-derived cells is not clear but they are absent in the 10-day-old postnatal mouse,

with the result that the terminal hindgut is aganglionic. Their presence in the terminal hindgut would appear to argue against our hypothesis of an E14.5 nonpermissive hindgut. However, putative changes in the gut environment might differ between the rostral and terminal portions of the middle region of colon so that vagal ENCCs do not progress, whereas the sacral crest cells might move. Nevertheless, the advance and morphology of sacral crest cells are not comparable to vagal ENCCs. The sacral-derived neural crest cells do not appear to invade the gut as multicellular strands but as single cells with long processes. Future investigations are necessary to clarify the migration and fate of these cells.

In conclusion, our studies show that the mutant colon becomes nonpermissive to ENCC invasion at a certain stage in development. Although our results clearly indicate a cell-autonomous role for EDNRB signaling in ENCCs, this does not preclude other non-autonomous effects or indirect consequences. Although the mutation is targeted only to NCCs, it is possible that the post-E14.5 environmental change is a consequence of this mutation and is not a normal physiological transition. Therefore, it will be important to determine whether aganglionic wild-type colon undergoes a similar change. Future experiments combining wild-type, and *Ednrb* conditional and total knockout mice will be used to determine whether the transition of the hindgut to a nonpermissive environment is a normal process.

Acknowledgements

The authors are grateful to Xiaoxiao Gu, Lance Rodenkirch, Dr John K. Harting, Alex Baumann and Joel Pulchaski for their support and encouragement. We are also grateful to Drs Raj Kapur and Don Newgreen for their comments on earlier versions of the manuscript and to Dr Amanda Barlow for her insightful suggestions. The UW Medical School Research Committee provided funding support for this study. This paper is dedicated to the memory of Marjorie Brothwell Hurie.

Supplementary material

Supplementary material for this article is available at <http://dev.biologists.org/cgi/content/full/136/18/3195/DC1>

References

- Alzahem, A. M. and Cass, D. T. (2008). *Animal Models of Aganglionosis in Hirschsprung's Disease and Allied Disorders* (ed. A. M. Holschneider and P. Puri), pp. 51-58. New York: Springer.
- Anderson, R. B., Newgreen, D. F. and Young, H. M. (2006). Neural crest and the development of the enteric nervous system. *Adv. Exp. Med. Biol.* **589**, 181-196.
- Bagnato, A., Rosano, L., Spinella, F., Di Castro, V., Tecce, R. and Natali, P. G. (2004). Endothelin B receptor blockade inhibits dynamics of cell interactions and communications in melanoma cell progression. *Cancer Res.* **64**, 1436-1443.
- Barlow, A., de Graaff, E. and Pachnis, V. (2003). Enteric nervous system progenitors are coordinately controlled by the G protein-coupled receptor EDNRB and the receptor tyrosine kinase RET. *Neuron* **40**, 905-916.
- Barlow, A. J., Wallace, A. S., Thapar, N. and Burns, A. J. (2008). Critical numbers of neural crest cells are required in the pathways from the neural tube to the foregut to ensure complete enteric nervous system formation. *Development* **135**, 1681-1691.
- Baynash, A. G., Hosoda, K., Giaid, A., Richardson, J. A., Emoto, N., Hammer, R. E. and Yanagisawa, M. (1994). Interaction of endothelin-3 with endothelin-B receptor is essential for development of epidermal melanocytes and enteric neurons. *Cell* **79**, 1277-1285.
- Bondurand, N., Natarajan, D., Barlow, A., Thapar, N. and Pachnis, V. (2006). Maintenance of mammalian enteric nervous system progenitors by SOX10 and endothelin 3 signalling. *Development* **133**, 2075-2086.
- Breau, M. A., Pietri, T., Eder, O., Blanche, M., Brakebusch, C., Fassler, R., Thiery, J. P. and Dufour, S. (2006). Lack of beta1 integrins in enteric neural crest cells leads to a Hirschsprung-like phenotype. *Development* **133**, 1725-1734.
- Burns, A. J., Champeval, D. and Le Douarin, N. M. (2000). Sacral neural crest cells colonize aganglionic hindgut in vivo but fail to compensate for lack of enteric ganglia. *Dev. Biol.* **219**, 30-43.
- Danielian, P. S., Echelard, Y., Vassileva, G. and McMahon, A. P. (1997). A 5.5-kb enhancer is both necessary and sufficient for regulation of Wnt-1 transcription in vivo. *Dev. Biol.* **192**, 300-309.
- de Graaff, E., Srinivas, S., Kilkenny, C., D'Agati, V., Mankoo, B. S., Costantini, F. and Pachnis, V. (2001). Differential activities of the RET tyrosine kinase receptor isoforms during mammalian embryogenesis. *Genes Dev.* **15**, 2433-2444.
- Delalande, J. M., Barlow, A. J., Thomas, A. J., Wallace, A. S., Thapar, N., Erickson, C. A. and Burns, A. J. (2008). The receptor tyrosine kinase RET regulates hindgut colonization by sacral neural crest cells. *Dev. Biol.* **313**, 279-292.
- Druckendrod, N. R. and Epstein, M. L. (2005). The pattern of neural crest advance in the cecum and colon. *Dev. Biol.* **287**, 125-133.
- Druckendrod, N. R. and Epstein, M. L. (2007). Behavior of enteric neural crest-derived cells varies with respect to the migratory wavefront. *Dev. Dyn.* **236**, 84-92.
- Druckendrod, N. R., Powers, P. A., Bartley, C. R., Walker, J. W. and Epstein, M. L. (2008). Targeting of endothelin receptor-B to the neural crest. *Genesis* **46**, 396-400.
- Garipey, C. E., Williams, S. C., Richardson, J. A., Hammer, R. E. and Yanagisawa, M. (1998). Transgenic expression of the endothelin-B receptor prevents congenital intestinal aganglionosis in a rat model of Hirschsprung disease. *J. Clin. Invest.* **102**, 1092-1101.
- Gershon, M. D. and Ratcliffe, E. M. (2004). Developmental biology of the enteric nervous system: pathogenesis of Hirschsprung's disease and other congenital dysmotilities. *Semin. Pediatr. Surg.* **13**, 224-235.
- Heanue, T. A. and Pachnis, V. (2007). Enteric nervous system development and Hirschsprung's disease: advances in genetic and stem cell studies. *Nat. Rev. Neurosci.* **8**, 466-479.
- Herbarth, B., Pingault, V., Bondurand, N., Kuhlbrodt, K., Hermans-Borgmeyer, I., Puliti, A., Lemort, N., Goossens, M. and Wegner, M. (1998). Mutation of the Sry-related Sox10 gene in Dominant megacolon, a mouse model for human Hirschsprung disease. *Proc. Natl. Acad. Sci. USA* **95**, 5161-5165.
- Hosoda, K., Hammer, R. E., Richardson, J. A., Baynash, A. G., Cheung, J. C., Giaid, A. and Yanagisawa, M. (1994). Targeted and natural (piebald-lethal) mutations of endothelin-B receptor gene produce megacolon associated with spotted coat color in mice. *Cell* **79**, 1267-1276.
- Jacobs-Cohen, R. J., Payette, R. F., Gershon, M. D. and Rothman, T. P. (1987). Inability of neural crest cells to colonize the presumptive aganglionic bowel of *ls/ls* mutant mice: requirement for a permissive microenvironment. *J. Comp. Neurol.* **255**, 425-438.
- Jiang, X., Rowitch, D. H., Soriano, P., McMahon, A. P. and Sucov, H. M. (2000). Fate of the mammalian cardiac neural crest. *Development* **127**, 1607-1616.
- Kapur, R. P., Livingston, R., Doggett, B., Sweetser, D. A., Siebert, J. R. and Palminter, R. D. (1996). Abnormal microenvironmental signals underlie intestinal aganglionosis in Dominant megacolon mutant mice. *Dev. Biol.* **174**, 360-369.
- Lahav, R. (2005). Endothelin receptor B is required for the expansion of melanocyte precursors and malignant melanoma. *Int. J. Dev. Biol.* **49**, 173-180.
- Landman, K. A., Simpson, M. J. and Newgreen, D. F. (2007). Mathematical and experimental insights into the development of the enteric nervous system and Hirschsprung's disease. *Dev. Growth Differ.* **49**, 277-286.
- Lane, P. W. (1966). Association of megacolon with two recessive spotting genes in the mouse. *J. Hered.* **57**, 29-31.
- Lange, K., Kammerer, M., Hegi, M. E., Grottegut, S., Dittmann, A., Huang, W., Fluri, E., Yip, G. W., Gotte, M., Ruiz, C. et al. (2007). Endothelin receptor type B counteracts tenascin-C-induced endothelin receptor type A-dependent focal adhesion and actin stress fiber disorganization. *Cancer Res.* **67**, 6163-6173.
- Maka, M., Stolt, C. C. and Wegner, M. (2005). Identification of Sox8 as a modifier gene in a mouse model of Hirschsprung disease reveals underlying molecular defect. *Dev. Biol.* **277**, 155-169.
- McCallion, A. S. and Chakravarti, A. (2001). EDNRB/EDN3 and Hirschsprung disease type II. *Pigment Cell Res.* **14**, 161-169.
- McCallion, A. S., Stames, E., Conlon, R. A. and Chakravarti, A. (2003). Phenotype variation in two-locus mouse models of Hirschsprung disease: tissue-specific interaction between Ret and Ednrb. *Proc. Natl. Acad. Sci. USA* **100**, 1826-1831.
- Nagy, N. and Goldstein, A. M. (2006). Endothelin-3 regulates neural crest cell proliferation and differentiation in the hindgut enteric nervous system. *Dev. Biol.* **293**, 203-217.
- Peters van der Sanden, M. J. H., Kirby, M. L., GittenbergerdeGroot, A., Tibboel, D., Mulder, M. P. and Meijers, C. (1993). Ablation of various regions within the avian vagal neural crest has differential-effects on ganglion formation in the foregut, midgut and hindgut. *Dev. Dyn.* **196**, 183-194.
- Sidebotham, E. L., Woodward, M. N., Kenny, S. E., Lloyd, D. A., Vaillant, C. R. and Edgar, D. H. (2002). Localization and endothelin-3 dependence of stem cells of the enteric nervous system in the embryonic colon. *J. Pediatr. Surg.* **37**, 145-150.
- Simpson, M. J., Zhang, D. C., Mariani, M., Landman, K. A. and Newgreen, D. F. (2007). Cell proliferation drives neural crest cell invasion of the intestine. *Dev. Biol.* **302**, 553-568.

- Srinivas, S., Watanabe, T., Lin, C. S., William, C. M., Tanabe, Y., Jessell, T. M. and Costantini, F.** (2001). Cre reporter strains produced by targeted insertion of EYFP and ECFP into the ROSA26 locus. *BMC Dev. Biol.* **1**, 4.
- Stanchina, L., Baral, V., Robert, F., Pingault, V., Lemort, N., Pachnis, V., Goossens, M. and Bondurand, N.** (2006). Interactions between Sox10, Edn3 and *Ednrb* during enteric nervous system and melanocyte development. *Dev. Biol.* **295**, 232-249.
- Webster, W.** (1973). Embryogenesis of the enteric ganglia in normal mice and in mice that develop congenital aganglionic megacolon. *J. Embryol. Exp. Morphol.* **30**, 573-585.
- Wu, J. J., Chen, J. X., Rothman, T. P. and Gershon, M. D.** (1999). Inhibition of in vitro enteric neuronal development by endothelin-3: mediation by endothelin B receptors. *Development* **126**, 1161-1173.
- Yanagisawa, H., Yanagisawa, M., Kapur, R. P., Richardson, J. A., Williams, S. C., Clouthier, D. E., de Wit, D., Emoto, N. and Hammer, R. E.** (1998). Dual genetic pathways of endothelin-mediated intercellular signaling revealed by targeted disruption of endothelin converting enzyme-1 gene. *Development* **125**, 825-836.
- Yntema, C. L. and Hammond, W. S.** (1954). The origin of intrinsic ganglia of trunk viscera from vagal neural crest in the chick embryo. *J. Comp. Neurol.* **101**, 515-541.
- Young, H. M., Bergner, A. J., Anderson, R. B., Enomoto, H., Milbrandt, J., Newgreen, D. F. and Whittington, P. M.** (2004). Dynamics of neural crest-derived cell migration in the embryonic mouse gut. *Dev. Biol.* **270**, 455-473.
- Young, H. M., Turner, K. N. and Bergner, A. J.** (2005). The location and phenotype of proliferating neural-crest-derived cells in the developing mouse gut. *Cell Tissue Res.* **320**, 1-9.